Title: Investigating Age-Related Decline in Sensorimotor Control Using Robotic Tasks
Abbreviated title: Robotic Assessment of Motor Aging

Laura Alvarez-Hidalgo[1], Ellie Edlmann[2], Gunnar Schmidtmann[3] & Ian S. Howard[1*]
[1] School of Computing, Engineering and Mathematics, University of Plymouth, Plymouth, Devon, United Kingdom.
[2] Peninsula Medical School (Faculty of Health), University of Plymouth, Plymouth, Devon, United Kingdom. ellie.edlmann@plymouth.ac.uk
[3] School of Health Professions (Faculty of Health), University of Plymouth, Plymouth, Devon, United Kingdom. gunnar.schmidtmann@plymouth.ac.uk

[*]Correspondence should be addressed to: ISH: ian.howard@plymouth.ac.uk
Telephone: +44 1752 586324

Journal Section: Behavioral/Cognitive
Number of pages: 28
Number of figures: 9
Number of tables: 7
Number of words for Abstract: 337
Number of words for Background: 548
Number of words for Discussion: 1582
Number of words for Conclusions: 201

Statement of Financial Interests or Conflicts of Interest: The authors declare that they have no financial, personal, or professional interests that could be construed to have influenced the paper.

Acknowledgements:
We thank the University of Plymouth Faculty of Health's Interdisciplinary Fellow Building Programme for financial support for this project. Financial support for this project for LAH was provided by the Engineering and Physical Sciences Research Council (EPSRC) and the University of Plymouth. Financial support for ISH, EE, and GS was provided by the University of Plymouth. During the preparation of this work, LAH and ISH utilized ChatGPT-4o for proofreading.

Keywords: Sensorimotor Control, Aging and Motor Function, Robotic Assessment, Motor Learning, Bimanual and Unimanual Coordination.

## Abstract (351/337)

Background:

Aging is linked to widespread changes in sensorimotor control, leading to functional decline, mobility limitations, and an increased risk of falls. Certain aspects of the neurological examination and assessment of the motor system are subjective, underscoring the need for objective and quantitative tools to evaluate sensorimotor performance.

Methods:
To address this, we designed three experimental tasks using the vBOT planar robotic manipulandum to compare sensorimotor performance in healthy young adults (<35 years) and older adults (>60 years). Unlike previous assessments, our tasks uniquely integrate simultaneous bimanual control and altered dynamic conditions to comprehensively assess sensorimotor capabilities. The first task involved a bimanual de novo motor learning paradigm in which participants coordinated both hands to control a virtual 2D arm and performed 400 center-out and out-to-center trials. The second task assessed unimanual control using the right hand to perform center-out movements to eight targets. It introduced dynamic forces simulating object manipulation during the final 200 trials. The third task was similar but applied a viscous force field in the last 200 trials. It also included a scoring mechanism rewarding brisk movements, thereby encouraging participants to perform closer to their maximum capabilities. In this task, performance was also compared between the dominant and non-dominant arms. Group comparisons and within-subject differences were evaluated using appropriate statistical analyses.

Results:
Each task effectively identified age-related differences, but the viscous resistance task proved particularly sensitive, capturing significant age-related declines in force generation and movement duration. This scoring approach likely amplified performance differences, highlighting its suitability for detecting subtle effects of aging.

Older adults generally showed slower movement, longer task completion times, reduced peak forces, and prolonged reaction times. However, individual performance varied, with some older participants performing on par with younger individuals. In the third experiment, the dominant arm showed consistently better performance than the non-dominant arm, underscoring the sensitivity of the metrics to lateralized differences in motor control.

Conclusions:
These findings suggest that robot-based tasks have potential to quantify age-related differences in sensorimotor control and may support more precise clinical assessments.

## Significance Statement (87/120)

This study utilizes a robotic manipulandum, i.e., the vBOT, to assess the effect of aging. Through precisely controlled repeatable sensorimotor tasks, we quantify movement characteristics in both younger and older adults, providing clear insights into age-related motor decline. Our approach not only highlights the magnitude and variability of functional changes with age but also establishes rigorous and reliable quantitative benchmarks that could serve as critical tools for evaluating preventative therapies. In turn, this could guide the development of interventions aimed at preserving motor performance in older age.

## News & Noteworthy (75/75)

This study introduces a novel approach to assessing how aging affects movement dynamics using a robotic system. As populations age, understanding sensorimotor decline becomes increasingly crucial. Unlike conventional assessments, our method quantifies motor control metrics with precision, revealing previously undetectable, subtle age-related changes in movement efficiency, reaction times, and force generation. This framework establishes a rigorous benchmark for evaluating age-related decline, offering valuable clinical applications and informing the design of interventions to support older adults.

## Background (548/650)

Over the past century, life expectancy has shown a steady increase. In 1920, the global average at birth was just 36.4 years; by 2020, it had more than doubled to 72.5 years. Due to this significant rise, combined with other factors, the population over the age of 60 is steadily expanding. By 2030, this age group is estimated to grow from 1 billion in 2019 to 1.4 billion, with projections suggesting it will further increase to 2.1 billion by 2050 (1,2). This growth in the aging population introduces a range of challenges, particularly in the context of health and associated age-related changes in human motor control.

With increasing life expectancy and a growing population of individuals over 60 years of age, it is important to investigate quantifiable sensorimotor indicators that signal the onset of age-related decline in healthy older adults. Identifying and measuring these early markers can equip health professionals with precise, objective, and reliable tools to assess sensorimotor function, decline and the extent of movement improvements resulting from therapy.

Pioneering work using robotic manipulanda, such as the MIT-Manus (3) and Kinarm (4) devices, has significantly advanced the quantitative assessment of sensorimotor performance during upper-limb movements. These robotic systems precisely measure and control limb dynamics and kinematics, enabling detailed examination of motor control strategies, sensory integration, and adaptation. The MIT-Manus has been instrumental in characterizing impaired motor function post-stroke, revealing deficits in movement smoothness, accuracy, and force control, which correlate closely with clinical evaluations of motor impairment (5,6). Similarly, the Kinarm robotic system has facilitated investigations into sensorimotor integration and proprioception, allowing researchers to isolate and quantify specific deficits in motor coordination and sensory processing after

neurological injuries or disorders (7). Robotic manipulanda provide precise and objective measurements, overcoming limitations of subjectivity and limited sensitivity inherent in traditional assessments.

Robotic manipulanda are extensively utilized to assess motor deficits associated with aging and various neurological conditions, providing objective, sensitive metrics beyond traditional clinical assessments. The high precision and repeatability of robotic measurements allow the early detection of subtle impairments in motor performance, which are characteristic of aging. Studies employing the Kinarm, for example, have identified age-related declines in proprioception, reaction time, and motor coordination, highlighting the subtle sensorimotor changes that precede overt functional deficits in older adults (8,9). Additionally, robotic assessments have been pivotal in evaluating the progression and severity of conditions like Parkinson's disease and multiple sclerosis, facilitating early diagnosis, monitoring disease progression, and assessing therapeutic efficacy with greater accuracy and reliability (10,11).

In the current study, we developed a set of experiments to systematically investigate age-related differences in sensorimotor control of the upper limb by employing a set of targeted experimental tasks using the vBOT robotic manipulandum (12). Specifically, we compared performance between healthy young adults (under 35 years) and older adults (over 60 years) across three distinct robotic tasks designed to assess both bimanual and unimanual sensorimotor capabilities. The tasks included coordinating both hands in a novel bimanual control scenario, as well as unimanual movements in altered force environments. Through these experiments, we aim to quantify age-related changes in key movement metrics - including movement speed, reaction time, and force output - to establish an objective and replicable framework for evaluating sensorimotor decline, thereby supporting potential improvements in clinical assessments targeting motor deficits associated with aging.

## Methods

To develop assessments suitable for future participants in a clinical setting, it was necessary to limit the duration of the tasks they would be required to perform. To ensure participants were not fatigued by the assessment procedure, we restricted the overall testing time to 30 minutes per assessment. Since the current study involves investigating the appropriateness of the assessments we were developing, we ran two experimental sessions per participant, although we envisage that running a single test session would be the goal in the future if the assessments are used for clinical purposes rather than research.

Participants: We recruited a total of 32 participants, consisting of 16 young adults and 16 older adults. Participants were screened to exclude individuals with a history of neurological conditions, musculoskeletal disorders, or significant visual impairments that could affect performance. Almost all participants took part in two separate experimental sessions. Half of the young adults and half of the older adults were randomly assigned to Experiments 1 and 2. Participants first completed Experiment 1, followed by Experiment

2. The remaining participants were assigned to Experiment 3. All but one of them completed it twice: once using the right arm and once using the left.

All participants were naïve to the objectives of the experiments and provided written informed consent prior to participation. Right-handedness was assessed using the Edinburgh Handedness Questionnaire (13), which confirmed that all participants were right-handed. All experiments followed the ethics protocol approved by the University of Plymouth's Faculty Research Ethics and Integrity Committee.

Experiments: We developed three different experiments. Experiment 1: Learning to Control a 2D Kinematic Arm, was a bimanual task that involved learning to control a two-dimensional (2D) virtual kinematic arm using both the left and right arms. Experiment 1 investigated 8 older adults (5 females and 3 males; mean age: 73.61 ± 6.24 years) and 8 younger adults (4 females and 4 males; mean age: 28.02 ± 2.92 years).

Experiment 2: Handle Mass Center-Out Movement, involved making unimanual right-handed point-to-point movements, initially in an unloaded null-field condition and later with a simulated mass at the handle. In Experiment 2, performance was investigated mainly reusing the same participants as in Experiment 1. It involved 8 older adults (5 females and 3 males; mean age: 73.61 ± 6.24 years) and 8 younger adults (3 females and 5 males; mean age: 28.69 ± 3.01 years).

Experiment 3: Handle Viscous Resistance Center-Out Movement, involved making unimanual point-to-point movements, initially in an unloaded null-field condition and later with simulated viscosity at the handle. In Experiment 3, almost all participants ran the task twice, once with each hand. The cohort used to investigate the effect of aging on right-hand performance included 8 older adults (4 females and 4 males; mean age: 69.09 ± 2.97 years) and 7 younger adults (4 females and 3 males; mean age: 22.42 ± 2.61 years). Left-hand performance was examined in all 7 younger adults and a smaller subset of 7 older participants, since one older participant was not available (leaving 4 females and 3 males; mean age: 68.35 ± 2.27 years).

**Apparatus:** Fig. 1 illustrates the experimental setup used in this study to analyze upper limb reaching movements. Participants interacted with a pair of vBOT robotic manipulanda (12). Each was equipped with a robotic handle that incorporated an activation switch, which participants needed to press during a trial to activate the controller and allow the experiment to proceed. During the experiment, participants were seated in a comfortable, cushioned chair and secured with two shoulder straps to reduce body movement. For the unimanual experiments, a participant's relevant forearm rested on an air sled, ensuring low-friction movement constrained to a 2D plane. For the bimanual experiments, both forearms were supported by air sleds. Throughout all experiments, participants could not directly observe their arms or hands; instead, veridical visual feedback was provided using a 2D virtual reality system, which displayed visual elements such as circles representing hand positions, target locations, and start points within the workspace.

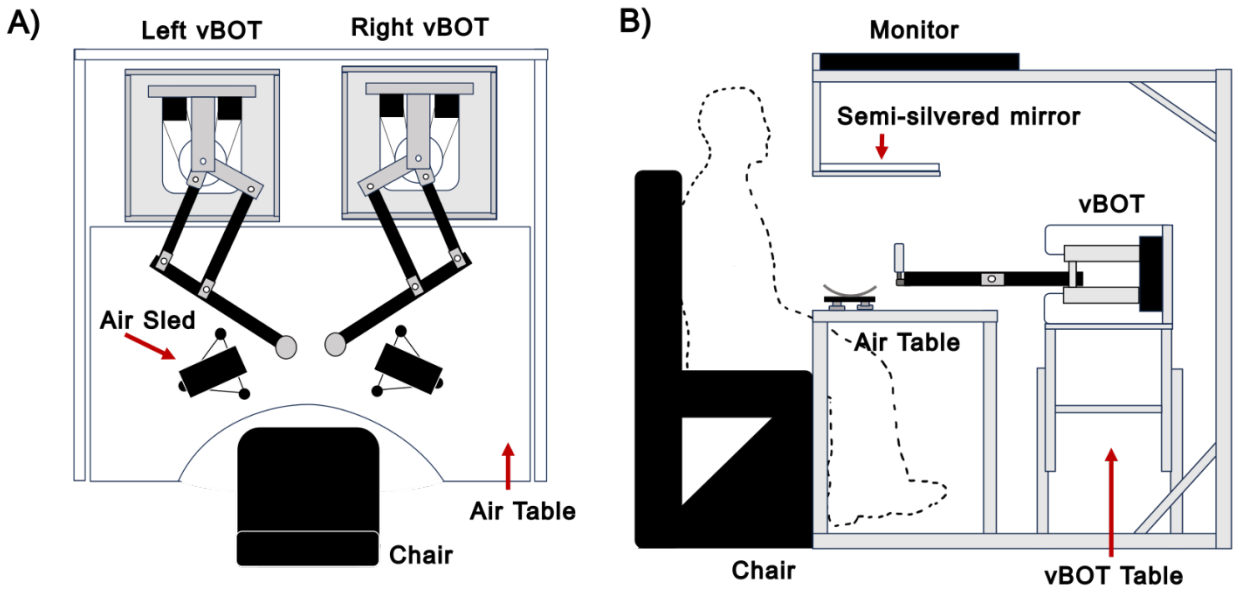


**Figure 1. Schematic Illustration of the vBOT Robotic Manipulandum. A:** Plan view of the vBOT robotic manipulandum setup. **B:** Side view of the vBOT robotic manipulandum setup.

Handle positions were measured using optical motor encoders, sampled at 1000 Hz, while torque-controlled motors generated endpoint forces. A force transducer (Nano 25; ATI), mounted beneath the left handle, measured the forces applied by participants during unimanual trials. These force signals were low-pass filtered at 500 Hz using 4th-order analog Bessel filters prior to digitization. Force and position data were stored for offline MATLAB analysis.

## Experiment 1: Learning to Control a 2D Kinematic Arm

In this experiment, participants were asked to perform movements by controlling a simulated two-link (2D) planar arm, as used in a study to investigate *de novo* learning (14). The experimental setup and design are shown in Fig. 2.

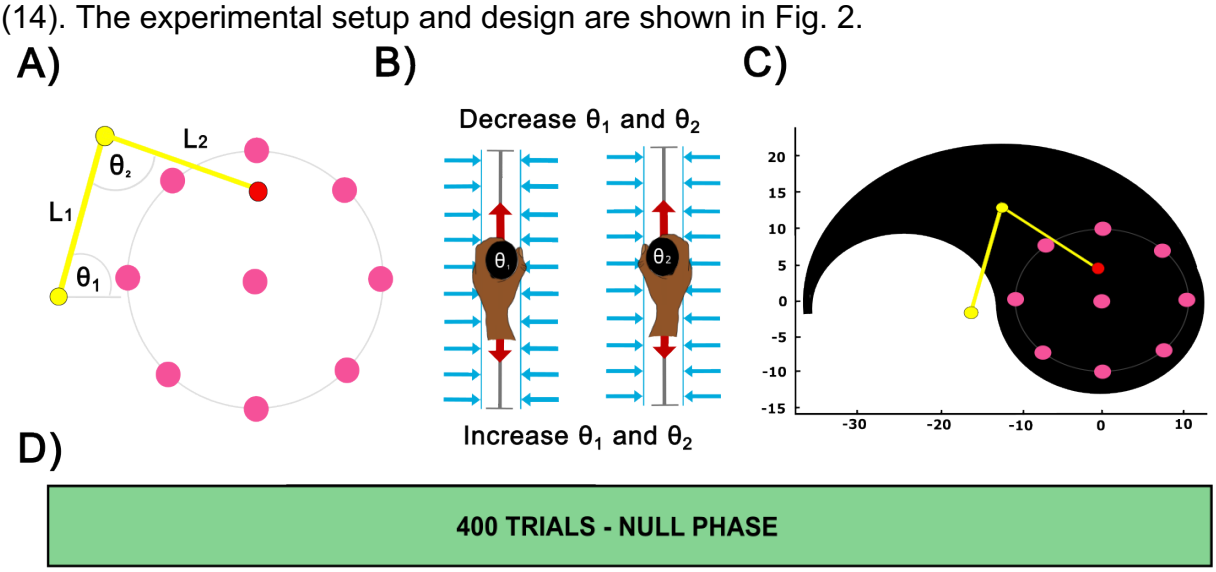

**Figure 2**. **Experiment 1: Learning to Control a 2D Kinematic Arm. A:** Experimental setup. Eight pink target points were arranged in a circular pattern at specific angular positions. The pink center point represents the starting position during center-out trials, and the target during out-to-center trials. A red cursor indicates the endpoint of a virtual 2D robotic arm with its links displayed in yellow. **B:** Dual-arm control mechanism. The left hand controls the joint angle $\theta_1$, and the right hand controls the joint angle $\theta_2$. **C:** The robotic arm's reachable workspace is shown in black, illustrating the range of motion for the virtual arm. **D:** Trial design. Each participant completed a total of 400 trials during the null-field phase.

## Virtual 2D Arm

Participants interacted with a simulated two-link robotic arm displayed in yellow, whose endpoint was represented by a red cursor. As shown in Fig. 2A, eight possible pink target points (radius: 1.0 cm) were arranged in a circular pattern at a radius of 10.8 cm from a central pink point (radius: 1.0 cm) and located at workspace origin (0,0). Targets were positioned at 0°, 45°, 90°, 135°, 180°, 225°, 270°, and 315°. The center point also served as the starting position for center-out trials and as the target for out-center trials.

Participants controlled the virtual 2D arm by grasping two robotic handles, each linked to a specific joint angle of the virtual 2D arm. The left handle controlled joint angle $\theta_1$, and the right handle controlled joint angle $\theta_2$, as depicted in Fig. 2B. Vertical hand movements adjusted these joint angles: upward movements decreased the angles, while downward movements increased them. To constrain hand movements to the y-axis, participants operated within two vertical channels (15).

## Trials Procedure

The experiment involved two types of movements: center-out movements and out-to-center movements. In center-out movement trials, participants started at the central position and moved the red cursor to one of the eight peripheral targets. In contrast, in out-to-center movement trials, participants started at a peripheral target and moved the red cursor back to the central position. Each trial began with the participant pressing both activation switches on the back of the robotic handles.

At the start of each center-out trial, the potential peripheral targets were first displayed in pink, while the central position appeared in grey. Participants then positioned the arm's endpoint cursor at the starting location. Once the cursor remained stationary at this location for 500 ms, the vBOT emitted an auditory cue (a beep). Simultaneously, one of the eight target locations was selected pseudorandomly and turned yellow, signaling the direction in which the participant should perform the trial. The virtual arm also appeared at this point. As the cursor moved out of the start location, the central grey point disappeared. The trial ended when the red cursor reached the target and stopped moving, at which point the virtual arm disappeared as well.

After completion of a center-out movement trial, participants performed an out-to-center trial, which returned the cursor to the central position. The procedure was similar to the

center-out trials, except the movement began at a peripheral location, and the central position turned yellow to indicate it as the target.

Experimental Block Design: As illustrated in Fig. 2D, the experiment consisted of 400 trials, divided into 25 blocks of 16 trials each. Each block included 8 center-out trials and 8 out-to-center trials.

Mechanical Channels: Participants' hand movements were constrained to two distinct vertical channels, each corresponding to one hand. These channels were aligned along the y-axis with a length of 30 cm (chanLen). Both channels were offset along the x-axis by ±10 cm from the center of the workspace, with the midpoints of the sliders located at (−10, 0) for the right hand and (+10, 0) for the left hand.

These linear channels were characterized by a stiffness value of 4,000 $Nm^{-1}$ ($k_{chan}$) and a damping coefficient of 30 $Nm^{-1}s$ ($b_{chan}$). The forces experienced by each hand within the channels were determined by the following equation, which relates the force to position and velocity:

$$\begin{bmatrix} F_{xh} \\ F_{yh} \end{bmatrix} = k_{chan} \begin{bmatrix} -1 & 0 \\ 0 & 0 \end{bmatrix} \begin{bmatrix} x_h \\ y_h \end{bmatrix} + b_{chan} \begin{bmatrix} -1 & 0 \\ 0 & 0 \end{bmatrix} \begin{bmatrix} \dot{x}_h \\ \dot{y}_h \end{bmatrix} \quad (1)$$

## Control of the Simulated Arm

The vertical position ($y$) of each handle was linearly scaled to map to the corresponding joint angle ($\theta$). This mapping was defined as:

$$\theta = \theta_{min} + (\theta_{max} - \theta_{min}) \frac{\left(dir_{slider} \cdot y + \frac{\text{chanLen}}{2}\right)}{\text{chanLen}} \quad (2)$$

For the left handle, the vertical position ($y_{h1}$) was mapped to a joint angle ($\theta_1$), within the range of $\theta_{min} = 0$ radians and $\theta_{max} = \pi$ radians. Similarly, the vertical position ($y_{h2}$) of the right handle was mapped to a joint angle ($\theta_2$), within the range of $\theta_{min} - \pi$ radians and $\theta_{max} = 0$ radians.

$$\theta_1 = \frac{(15 - y_{h1})}{30}\pi \quad (3) \qquad \theta_2 = \frac{(15 - y_{h2})}{30}\pi - \pi \quad (4)$$

This allowed the y-position of the handles to be effectively converted into joint angles within their respective ranges.

## Simulating Forward Kinematics

To compute the endpoint and visualize the configuration of the 2D arm, its forward kinematics were used. The simulated arm link lengths $l_1$ and $l_2$ were both 16.2 cm long. By employing trigonometric analysis, the positions of the elbow and end effector in Cartesian coordinates can be described using matrix equations:

$$\begin{bmatrix} x_{elbow} \\ y_{elbow} \end{bmatrix} = \begin{bmatrix} l_1 \cos(\theta_1) \\ l_1 \sin(\theta_1) \end{bmatrix} + \begin{bmatrix} x_{shoulder} \\ y_{shoulder} \end{bmatrix} \tag{5}$$

$$\begin{bmatrix} x_{end} \\ y_{end} \end{bmatrix} = \begin{bmatrix} l_1 \cos(\theta_1) + l_2 \cos(\theta_1 + \theta_2) \\ l_1 \sin(\theta_1) + l_2 \sin(\theta_1 + \theta_2) \end{bmatrix} + \begin{bmatrix} x_{shoulder} \\ y_{shoulder} \end{bmatrix} \tag{6}$$

The shoulder position (-12, -2) was located slightly below the central start location and to its left just outside the circle on which the targets are located.

## Experiment 2: Handle Mass Center-Out Movement

This experiment investigated participants' ability to perform center-out movements under two conditions: in a null-field allowing free movement, and in a condition simulating the effect of moving a 5 kg mass located at the handle. The experimental design is summarized in Fig. 3.

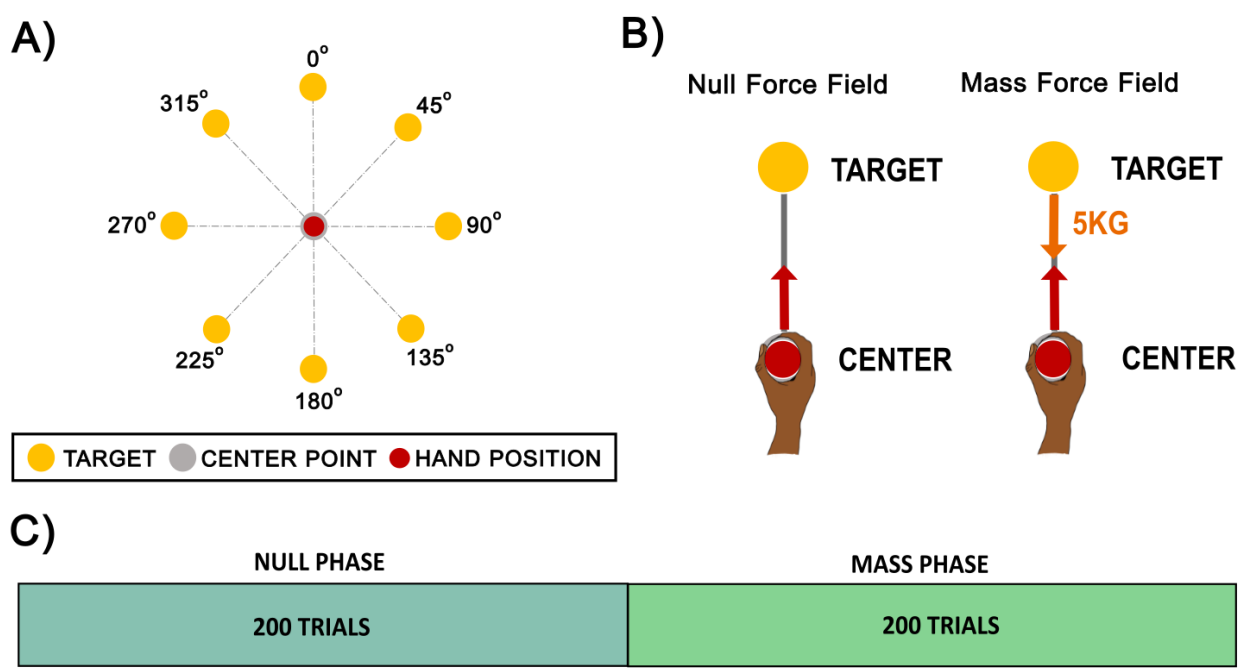


**Figure 3. Experiment 2: Handle Mass Center-Out Movement. A:** Experimental setup. Eight yellow targets were arranged at specific angular locations. A grey center point represented the starting position, while a red cursor indicated the participant's hand

location. **B:** Experimental phases. Participants experienced either a null-field, allowing free movement within the workspace, or the effect of a mass. The latter introduced inertial resistance by simulating the sensation of moving a 5 kg point mass around the workspace. **C:** Experimental conditions. The experiment consisted of 400 trials in total: 200 trials in the null-field phase, followed by 200 trials in the point mass phase.

## Experimental Setup

Participants were instructed to perform center-out movements toward one of eight possible yellow targets positioned in a circular pattern around a grey center point. As depicted in Fig. 3A, the starting position was represented by a central grey circle (radius: 1.25 cm) at the center of the workspace (0,0), and a red cursor (radius: 0.5 cm) displayed the hand's position in the workspace. Additionally, eight yellow target circles (radius: 0.5 cm) were arranged in a circular pattern at a radius of 12 cm from the center, located at angular positions of 0º, 45º, 90º, 135º, 180º, 225º, 270º, and 315º. Only one target appeared on the screen at a time.

Participants controlled the red cursor by holding the left vBOT robotic handle. At the start of each trial, participants viewed an empty screen and grasped the left vBOT robotic handle. The vBOT guided their hand to the designated center position. After remaining stationary at this location for 300 ms, an auditory beep signaled the beginning of the trial. At the same time, the hand position cursor, as well as a single yellow target, appeared on the screen. At this point, participants were required to move their hand from the center position toward the displayed target. The trial concluded when the participant successfully reached the target.

## Experimental Block Design

Movements were undertaken under two conditions. During this center-out movement, participants encountered either a null-field or a 5 kg mass (see Fig. 3B). Each condition consisted of 400 trials, with the first 200 conducted in a null-field phase and the remaining 200 in an endpoint mass phase. Approximately midway through the experimental condition, participants were given a 10-second rest. However, participants could take a break at any time simply by releasing the activation switch. The timeline of trials is shown in Fig. 3C.

## Simulating Mass

To ensure a stable simulation, moving the mass was modeled as being connected to the hand cursor via a stiff spring. Additionally, viscous damping was incorporated in the simulation, to enhance stability. At the start of the simulation, the mass' position is initialized to match the current location of the hand cursor. The mass' velocity, acceleration, and the forces acting on it are all set to zero.

$$\begin{bmatrix} x_m \\ y_m \end{bmatrix} = \begin{bmatrix} x_{cur} \\ y_{cur} \end{bmatrix} \tag{7}$$

$$\begin{bmatrix} v_{xm} \\ v_{ym} \end{bmatrix} = \begin{bmatrix} 0 \\ 0 \end{bmatrix} \tag{8}$$

$$\begin{bmatrix} a_{xm} \\ a_{ym} \end{bmatrix} = \begin{bmatrix} 0 \\ 0 \end{bmatrix} \tag{9}$$

$$\begin{bmatrix} F_{xm} \\ F_{ym} \end{bmatrix} = \begin{bmatrix} 0 \\ 0 \end{bmatrix} \tag{10}$$

Within the main simulation update loop, which operates at a nominal frequency of 1 kHz, the motion of the mass is updated in real time. At each time step, the position of the mass is updated using Euler integration based on its velocity:

$$\begin{bmatrix} x_m \\ y_m \end{bmatrix} = \begin{bmatrix} x_m \\ y_m \end{bmatrix} + \begin{bmatrix} v_{xm} \\ v_{ym} \end{bmatrix} \mathrm{Dt} \tag{11}$$

Here, $\mathrm{Dt}$ represents the timestep since the last update, typically 1 ms. The mass' acceleration is then calculated using the following equation:

$$\begin{bmatrix} a_m \\ a_m \end{bmatrix} = \frac{1}{m} \begin{bmatrix} F_{xm} \\ F_{ym} \end{bmatrix} \tag{12}$$

where m = 5 kg is the mass and $\begin{bmatrix} F_{xm} \\ F_{ym} \end{bmatrix}$ is the force acting on it. Using Euler integration, the velocity of the mass is updated based on its acceleration:

$$\begin{bmatrix} v_{xm} \\ v_{ym} \end{bmatrix} = \begin{bmatrix} v_{xm} \\ v_{ym} \end{bmatrix} + \begin{bmatrix} a_{xm} \\ a_{ym} \end{bmatrix} \mathrm{Dt} \tag{13}$$

The force acting on the mass is determined by the extension of the spring, which connects the mass to the endpoint of the arm. The spring has a stiffness constant of $k_{mass}$ = 2000 N/m:

$$\begin{bmatrix} F_{xm} \\ F_{ym} \end{bmatrix} = -k_{mass} \left( \begin{bmatrix} x_m \\ y_m \end{bmatrix} - \begin{bmatrix} x_{end} \\ y_{end} \end{bmatrix} \right) \tag{14}$$

The endpoint velocity, which is directly available from the handle velocity, is used to calculate an additional viscous damping force for further stability enhancement. The viscous damping force is given by:

$$\begin{bmatrix} F_{xdamp} \\ F_{ydamp} \end{bmatrix} = -b_{end} \begin{bmatrix} \dot{x}_{end} \\ \dot{y}_{end} \end{bmatrix} \tag{15}$$

Here, the damping viscosity coefficient ($b_{end}$) is 10 $Nm^{-1}s$. Finally, the spring force (Eq. 14) and damping force (Eq. 15) are combined to compute the total force experienced at the handle.

## Experiment 3: Handle Viscous Resistance Center-Out Movement

This experiment was similar to Experiment 2. However, after the initial 200 trials, during the second phase of the experiment, instead of introducing a 5 kg simulated point mass at the handle, a viscous force field that resisted hand movement was introduced. This resistance was proportional to the velocity of movement, producing a sensation similar to moving underwater. The experimental design is illustrated in Fig. 4.

Experiment 3 was first carried out with their right hand. To compare dominant and non-dominant arm movement performance, some participants also repeated the experiment with their left hands.

## Viscous Force Field

To implement viscous resistance in the direction of movement, we used the force equation:

$$\mathrm{F} = -\eta v \tag{16}$$

Where the viscous-field constant $\eta$ has a value of 0.3 N.s/m.

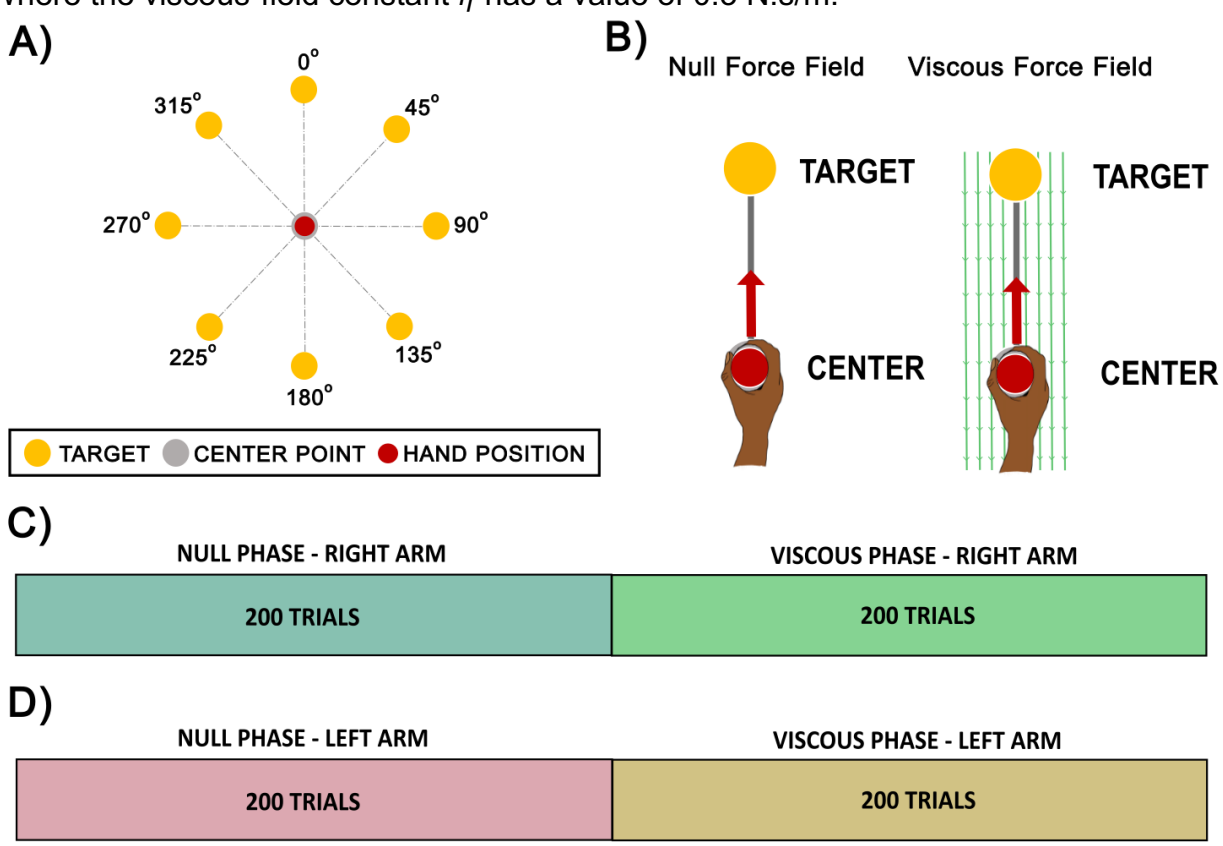

**Figure 4. Experiment 3: Handle Viscous Resistance Center-Out Movement. A:** Experimental setup. Eight yellow targets were arranged at specific angular locations. A grey center point represented the starting position, while a red cursor displayed the participant's hand location. **B:** Experimental phases. Participants experienced either a null-field, allowing free movement within the workspace, or a viscous-field, which introduced resistance. **C:** Right-Hand Experimental Condition. Participants performed the experiment with their right arm for all 400 trials: 200 trials in a null-field phase, followed by 200 trials in a viscous-field phase. **D:** Left-Hand Experimental Condition. Participants repeated the same experimental procedure performed with their right hand, but this time using their left hand.

### Experimental Block Design

Each condition consisted of 400 trials, with the first 200 conducted in a null-field phase and the remaining 200 in a viscous force-field phase. Approximately midway through the experimental condition, participants were given a 10-second rest period. Participants could also take a break at any time simply by releasing the activation switch. The timeline of trials to assess right-hand performance is shown in Fig. 4C. In this experiment, participants received a score reflecting the number of times they achieved a brisk movement, thereby encouraging them to move faster than they otherwise might have done.

### Dominant verses Non-Dominant Arm Usage

To assess how dominant verses non-dominant arm use affects performance on movement characteristics and performance, each participant performed the experiment twice: once using their right arm and once using their left arm (refer to Fig. 4D). This also provided an effective means to examine the robustness of the movement analyses, as it permitted intra-participant comparisons that were unaffected by the different levels of performance that occur across participants.

## Data Analysis

The experimental data was processed offline using MATLAB R2024a. For the de novo arm experiment (Experiment 1), we examined the trajectory of the cursor, which corresponded to the endpoint of the virtual arm. For the null-mass experiment (Experiment 2) and the null-viscous experiment (Experiment 3), we also examined the trajectory of the cursor, which corresponded to the location of the robot handle.

Each trial began with an auditory cue (a beep). Movement onset was defined as the moment the hand exceeded a distance of 1.25 cm from the starting position and its speed surpassed 5 cm/s. Movement termination was defined as the moment the hand entered within 1.25 cm of the target and its speed dropped below 5 cm/s.

## Hand Trajectory Plots

For the de novo arm experiment (Experiment 1) we plot the mean ± standard error (SE) of movement trajectories over the first and final blocks of trials to provide an intuitive visualization of participants' movement behavior.

## Performance Metrics

We quantified kinematic accuracy with six metrics:

Absolute Maximum Perpendicular Error (AMPE): For each trial, we computed the absolute maximum perpendicular deviation of the movement trajectory from the ideal straight line connecting the start and target cursor locations in extrinsic space. By taking the absolute value, this metric avoids positive and negative deviations from canceling each other out across trials and provides a clear overall measure of how accurately participants followed a straight path from the starting point to the target.

**Movement Duration:** The time taken to complete a movement was calculated as the difference between the movement onset and termination times.

**Movement Length:** The total path length was determined by summing the distances between consecutive (x, y) cursor positions along the trajectory, from movement start to movement end.

**Reaction Time:** The time elapsed between the cue to start moving and actual movement onset.

**Maximum Speed:** The highest speed attained during the movement.

**Maximum Force:** The peak force exerted in the direction of movement.

## Statistical Analysis

Statistical analyses were performed using JASP software (16). When appropriate, Mauchly's test was applied to assess the assumption of sphericity. If this assumption was violated, Greenhouse-Geisser corrections were used to adjust the degrees of freedom. The significance level ($\alpha$) was set at 0.05 for all tests. Omega squared ($\omega^2$) was reported as a measure of effect size, indicating the proportion of variance in the dependent variable explained by the independent variables.

Repeated measures ANOVAs were used to examine differences in key metrics across critical phases within each experimental condition. When a significant main effect was observed, where appropriate we proceeded with post hoc comparisons using the Holm-Bonferroni correction. Bonferroni-corrected p-values are indicated as pBonf.

To compare metrics across the conditions, of age (younger verses older participants and the use of the right verses left hand), separate ANOVAs were conducted on the initial

exposure metrics (defined as the mean of the first 25 exposure blocks) and the final exposure metrics (mean of the last 25 exposure blocks).

## Results

### Experiment 1: Learning to Control a 2D Kinematic Arm.

The first experiment was a novel bimanual kinematic arm task in which participants controlled the endpoint of a simulated two-dimensional (2D) arm to complete a center-out task. Their left- and right-hand positions, restricted to vertical movements, determined the arm's joint angles. The experiment consisted of a total of 400 trials.

Fig. 5 shows the mean and standard error (SE) of both outwards and inwards endpoint movement trajectories of the virtual arm at two critical stages, for both younger and older participants. Panel A illustrates the first 16 trials of the younger participants, where movements are highly erratic, reflecting exploratory behavior as they attempt to gain control of the arm's endpoint. By the end of the experiment, as shown in Panel B, trajectories become much straighter, and deviations from the mean direction are markedly reduced. Similar improvements are observed in older participants. Panel C displays the first 16 trials for the older group, also showing highly erratic movements. However, by the end of the 400 trials, their performance improves significantly as well. Qualitatively, younger participants appear to perform slightly better than older participants, in terms of the straightness of their movements. We also note that for both sets of participants, inward movements were straighter than outward movements, no doubt arising from the fact that it was easier to move back to the central location than outwards to one of many peripheral targets.

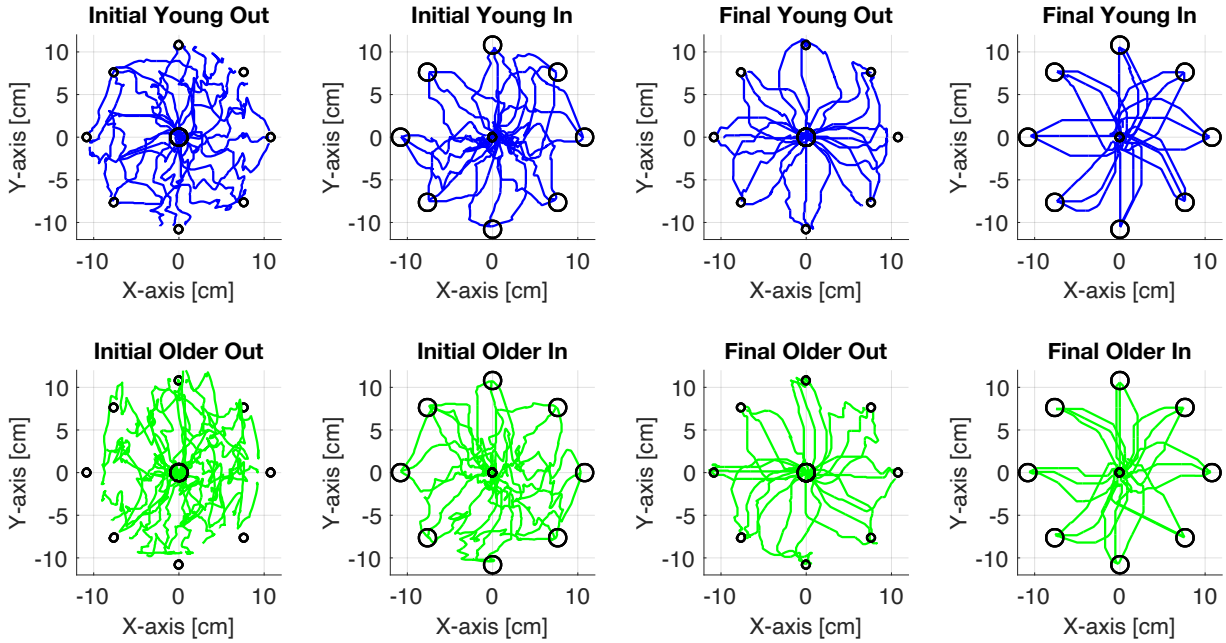

**Figure 5.** Plots showing the mean ± standard error (SE) of virtual arm endpoint trajectories over 16 trials for outward and inward movements: A: Under-35 years, initial trials (1 - 16); B: Under-35 years, final trials (385–400); C: Over-60 years, initial trials (1–16); D: Over-60 years, final trials (385–400).

Behavioral trends related to age were evident in the kinematic arm task data. Younger adults, in general, took less time to complete each trial and made straighter movements in extrinsic space. These quantitative indicators of motor performance across age groups may serve as a means for evaluating the effectiveness of future rehabilitation strategies.

Fig. 6 displays movement metrics used to quantify the performance of the endpoint movement of the virtual arm. Each metric represents the average of 16 consecutive trials and is plotted against block pairs. Across all metrics, there is a general tendency for performance to improve with trial number. Panel A shows that movement duration starts ~~off~~ high for both younger and older participants but decreases considerably by the end of the 400 trials. Younger participants exhibit consistently shorter movement durations than older participants. Panel B presents the absolute maximum perpendicular error (AMPE) across block pairs, with a general downward trend. Younger participants tend to show slightly lower AMPE values compared to older participants. Panel C depicts reaction time - defined as the interval between the cued start of a trial and movement initiation. Younger participants consistently demonstrate shorter reaction times. Panel D shows the maximum movement speed as a function of block pair, revealing a slight overall increase with practice. Younger participants move faster than older participants on average. Panel E displays trajectory path length, which is consistently shorter in younger participants across all trial blocks.

## Comparisons of results within age group and conditions

Repeated-measures ANOVAs were used to examine whether there were any significant variations in the measured metrics across the initial and final two blocks (32 trials) for both younger and older participants.

Both younger and older participants showed significant changes over time in Duration, AMPE, Reaction Time, and Path Length, with large effect sizes across all four metrics. Reaction Time showed particularly large effects, especially in older adults ($\omega^2 = 0.664$). No significant changes were observed in Peak Speed for either group. Detailed results are summarized in Table 1.

**Table 1.** Repeated-measures ANOVA results for each age group across the entire experiment: Separate repeated-measures ANOVAs were conducted for each performance metric to assess overall changes across the full duration of the task within each age group. Reported values include F-statistics, p-values, and effect sizes ($\omega^2$). Significant p-values are shown in bold.

| AGE GROUP | METRIC | F | P | $\omega^2$ |
|---|---|---|---|---|
| Younger | Duration | 35.808 | **< 0.001** | 0.643 |

| | | | | |
|---|---|---|---|---|
| | AMPE | 20.611 | **0.003** | 0.460 |
| | Reaction Time | 22.820 | **0.002** | 0.530 |
| | Peak Speed | 0.014 | 0.909 | 0.000 |
| | Path Length | 25.384 | **0.001** | 0.546 |
| Older | Duration | 44.317 | **< 0.001** | 0.741 |
| | AMPE | 39.080 | **< 0.001** | 0.546 |
| | Reaction Time | 107.030 | **< 0.001** | 0.664 |
| | Peak Speed | 0.121 | 0.738 | 0.000 |
| | Path Length | 19.747 | **0.003** | 0.482 |

**Summary within age group and conditions**

The repeated-measures ANOVAs revealed some significant improvements in task performance across training for both younger and older participants. Specifically, Duration, Absolute Mean Position Error (AMPE), Reaction Time, and Path Length all significantly decreased from the initial to the final blocks of training, indicating enhanced movement efficiency and response preparation over time. In the younger group, all four metrics showed marked improvements with large effect sizes, such as $\omega^2 = 0.643$ for Duration. Similarly, the older group demonstrated significant gains, with particularly strong effects observed for Reaction Time ($F = 107.303$, $p < 0.001$, $\omega^2 = 0.664$). Overall, the results demonstrate clear learning effects within both age groups, with improvements across multiple performance metrics except for Peak Speed.

**Comparisons of Results Across Age Group Conditions**

To investigate age-related differences in performance, we compared average values for each metric between younger and older participants using an ANOVA, analysing the first half of trials (1–200) and the second half (201–400) separately.

During Phase 1, no significant age-related differences were observed, though Duration showed a trend toward significance with a moderate effect size ($\omega^2 = 0.131$). In Phase 2, significant differences were found in Duration ($p = 0.008$, $\omega^2 = 0.343$) and Reaction Time ($p = 0.041$, $\omega^2 = 0.202$), indicating that older participants performed slower and responded more slowly in the later stage of the task. No differences were found in AMPE, Peak Speed, or Path Length. Detailed results are summarized in Table 2.

**Table 2.** ANOVA results comparing younger and older participants within each experimental phase**:** Separate one-way ANOVAs were conducted for each performance metric during Phase 1 (P1, trials 1–200) and Phase 2 (P2, trials 201–400). Reported values include F-statistics, p-values, and effect sizes ($\omega^2$). Significant p-values are shown in bold.

| PHASE OF EXPERIMENT | METRIC | F | P | $\omega^2$ |
|---|---|---|---|---|
| P1 | Duration | 3.419 | 0.086 | 0.131 |

| | | | | |
|---|---|---|---|---|
| | AMPE | 0.186 | 0.673 | 0.000 |
| | Reaction Time | 1.838 | 0.197 | 0.050 |
| | Peak Speed | 0.679 | 0.424 | 0.000 |
| | Path Length | 0.997 | 0.335 | 0.000 |
| P2 | Duration | 9.367 | **0.008** | 0.343 |
| | AMPE | 0.296 | 0.595 | 0.000 |
| | Reaction Time | 5.038 | **0.041** | 0.202 |
| | Peak Speed | 0.565 | 0.465 | 0.000 |
| | Path Length | 0.980 | 0.339 | 0.000 |

**Summary cross age**

In the first half, there were no significant differences between age groups for any of the measures. In the second half of trials, only movement Duration and Reaction Time are significantly shorter in the younger participants (p = 0.008 and p = 0.041, respectively). No other metrics showed a statistically significant difference between the two age groups.

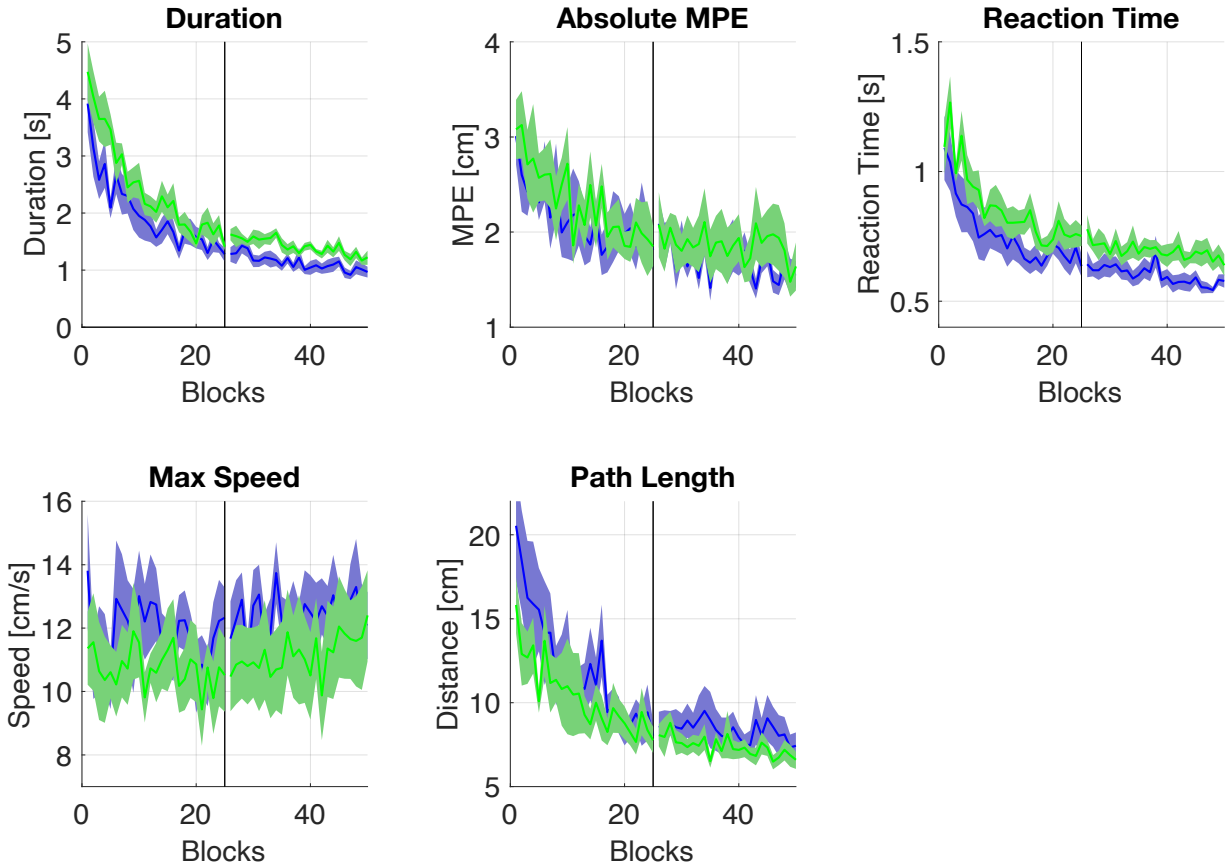


**Figure 6.** Movement metrics quantifying the trajectory at the endpoint of the virtual arm, plotted against block pairs. Younger participants are plotted in blue, and older participants are plotted in green. **A:** Duration of movement. **B:** Absolute maximum perpendicular error (AMPE). **C:** Movement reaction time. **D:** Maximum trajectory speed. **E:** Trajectory path length.

## Experiment 2: Handle Mass Center-Out Movement

The second experiment was a right-hand center-out task involving two field conditions: a null field and a simulated endpoint mass. Participants made 12 cm movements from a central starting position to one of eight targets in each of two 200-trial phases.

The conditions were designed to investigate performance during unloaded and loaded movements. Behavioral trends related to age were evident: younger adults typically made faster, shorter-duration movements, generated greater peak forces in the direction of movement, and exhibited quicker reaction times.

Fig. 7 shows the performance of younger and older participants across several metrics quantifying hand trajectories during the null-mass center-out task. Compared to the older participants, younger participants take less time to complete the movement, have a faster reaction time, move with a higher peak speed, generate more force in the direction of movement, and have shorter path lengths. However, AMPE is quite similar across the groups.

### Comparisons of results within age group and conditions

Repeated-measures ANOVAs were used to examine the significance of differences in the measured metrics between pairs of blocks (16 trials each) located at the initial null exposure, final null exposure, initial mass dynamic exposure, and final mass dynamic exposure. Post hoc comparisons were conducted to further assess significant differences between these phases.

Significant phase effects were observed in several performance metrics for both age groups. Bonferroni-corrected post hoc tests showed that the introduction of the mass dynamic ($p_{Bonf}$ 2) led to consistent performance changes in AMPE, Peak Speed, Peak Y-Force, and Path Length for younger participants, and in Duration, AMPE, Reaction Time, and Path Length for older participants. Adaptation across the mass dynamic phase ($p_{Bonf}$ 3) was evident primarily in AMPE and Path Length in both groups. Only older participants exhibited significant changes in Reaction Time. Path Length showed the largest effect sizes in both groups, indicating strong sensitivity to dynamic perturbation. Detailed results are summarized in Table 3.

**Table 3.** Repeated-measures ANOVA results for each age group across task phases: Each metric was analyzed using repeated-measures ANOVAs to assess changes across three task transitions: (1) from the initial to final null blocks, (2) from the final null blocks to the introduction of the mass dynamic, and (3) from the start to the end of the mass dynamic blocks. The table presents F-statistics, p-values, effect sizes ($\omega^2$), and Bonferroni-corrected post hoc p-values for each comparison. Significant p-values are shown in bold.

| AGE GROUP | METRIC | F | P | $\omega^2$ | $P_{BONF}$ (1) | $P_{BONF}$ (2) | $P_{BONF}$ (3) |
|---|---|---|---|---|---|---|---|

| | | | | | | | |
|---|---|---|---|---|---|---|---|
| Younger | Duration | 21.168 | **< 0.001** | 0.539 | 0.244 | **< 0.001** | 0.077 |
| | AMPE | 18.210 | **< 0.001** | 0.493 | 0.009 | **0.017** | **0.003** |
| | Reaction Time | 5.227 | **0.007** | 0.165 | 0.158 | 0.118 | 0.914 |
| | Peak Speed | 6.705 | **0.002** | 0.161 | 1.000 | **< 0.001** | 0.094 |
| | Peak Y-Force | 26.530 | **< 0.001** | 0.608 | 1.000 | **0.011** | 1.000 |
| | Path Length | 40.052 | **< 0.001** | 0.649 | 0.305 | **< 0.001** | **0.001** |
| Older | Duration | 17.697 | **< 0.001** | 0.398 | **0.030** | **0.001** | **0.006** |
| | AMPE | 9.258 | **< 0.001** | 0.384 | 0.155 | **0.009** | **0.017** |
| | Reaction Time | 6.113 | **0.004** | 0.129 | 0.947 | **0.026** | **0.003** |
| | Peak Speed | 5.860 | **0.005** | 0.058 | 0.087 | 0.124 | 1.000 |
| | Peak Y-Force | 20.825 | **< 0.001** | 0.519 | 1.000 | **0.013** | 0.663 |
| | Path Length | 55.636 | **< 0.001** | 0.776 | 0.310 | **< 0.001** | **0.001** |

**Summary within age group and conditions**

For younger participants, AMPE decreased significantly by the end of the null blocks, increased with the introduction of the mass dynamic, and decreased again by its end. Duration and Peak Speed increased significantly with the mass dynamic but did not change significantly otherwise. Peak Y-Force and Path Length also increased significantly with the mass dynamic; Path Length then decreased significantly by the end of this phase. Reaction Time showed no significant changes.

For older participants, Duration decreased significantly during the null phase, increased with the mass dynamic, and decreased again by its end. AMPE and Reaction Time both increased significantly with the mass dynamic and decreased significantly by its end. Peak Y-Force and Path Length increased significantly with the mass dynamic, and Path Length also decreased significantly by the end of this phase. Peak Speed showed no significant changes.

Compared to younger participants, older participants showed significant changes in Reaction Time and Duration across all phases, indicating a broader sensitivity to the mass dynamic. In contrast, younger participants showed no significant changes in Reaction Time and more selective effects, with AMPE showing the clearest pattern of adaptation.

**Cross-age statistical analyses**

To investigate age-related differences in performance, we compared average values for each metric between younger and older participants using an ANOVA, analysing the first half of trials (1–200) and the second half (201–400) separately.

In Phase 1, significant age-related differences were observed in Duration, Peak Speed, and Path Length (all $p < 0.05$), with moderate to large effect sizes. Differences in Reaction Time and Peak Y-Force approached significance. In Phase 2, only Reaction Time

reached the conventional threshold for significance (p = 0.050), with a moderate effect size ($\omega^2$ = 0.184). Detailed results are summarized in Table 4.

**Table 4.** ANOVA results comparing younger and older participants within each experimental phase: Separate one-way ANOVAs were conducted for each metric within Phase 1 (P1, trials 1–200) and Phase 2 (P2, trials 201–400). Reported values include F-statistics, p-values, and effect sizes ($\omega^2$). Significant p-values are shown in bold.

| PHASE OF EXPERIMENT | METRIC | F | P | $\omega^2$ |
|---|---|---|---|---|
| P1 | Duration | 5.779 | **0.031** | 0.230 |
| | AMPE | 0.643 | 0.436 | 0.000 |
| | Reaction Time | 3.767 | 0.073 | 0. 147 |
| | Peak Speed | 5.640 | **0.032** | 0.225 |
| | Peak Y-Force | 4.185 | 0.060 | 0.166 |
| | Path Length | 7.950 | **0.014** | 0.303 |
| P2 | Duration | 3.721 | 0.074 | 0.145 |
| | AMPE | 0.021 | 0.886 | 0.000 |
| | Reaction Time | 4.601 | 0.050 | 0.184 |
| | Peak Speed | 3.141 | 0.098 | 0.118 |
| | Peak Y-Force | 2.929 | 0.109 | 0.108 |
| | Path Length | 2.833 | 0.114 | 0.103 |

## Summary cross-age

In the null phase movement duration is significantly shorter in the younger participants (*p* = 0.031), who also exhibit higher peak speed (p=0.032) and longer path lengths (*p* = 0.014). No other metrics showed a statistically significant difference between the two age groups.

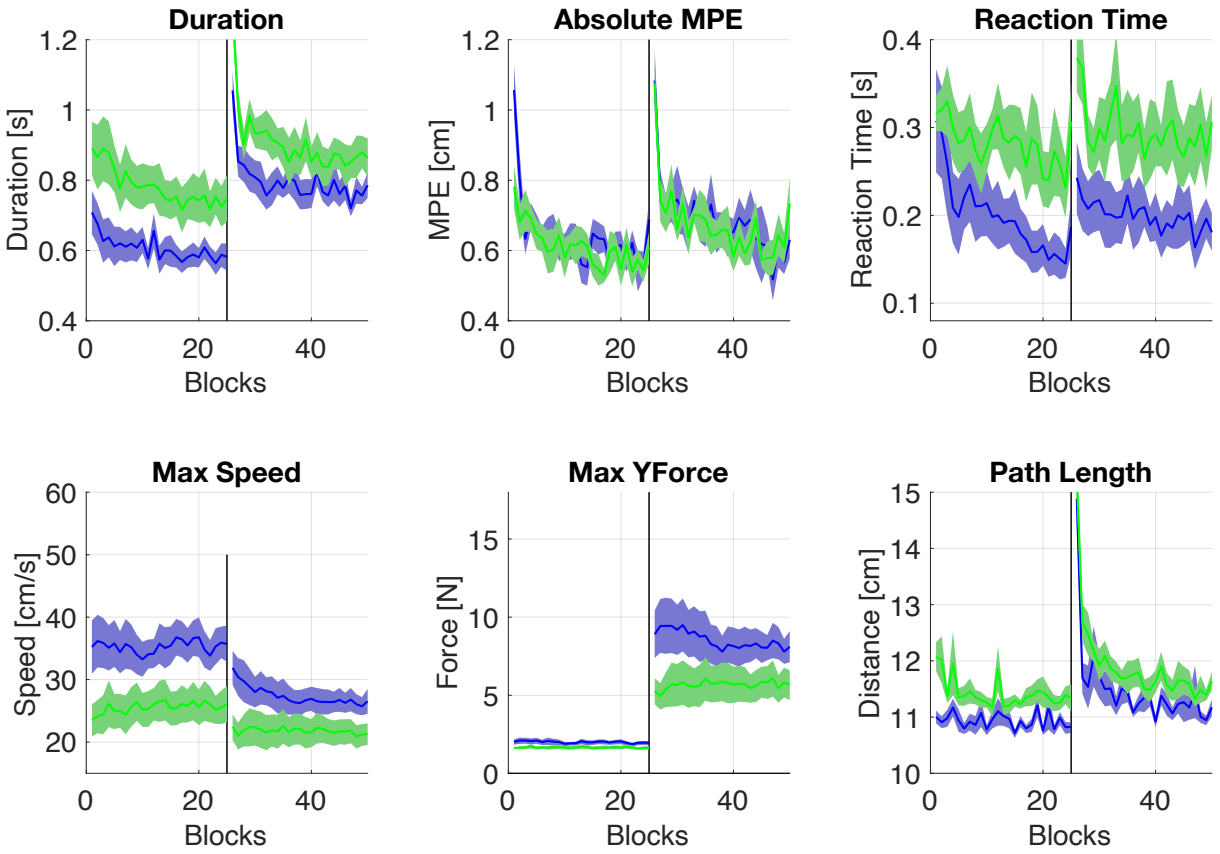


**Figure 7. Movement metrics quantifying the hand trajectory during the null-mass center-out task, plotted against blocks**. Younger participants are shown in blue, and older participants in green. **A:** Movement duration. **B:** Absolute maximum perpendicular error (AMPE). **C:** Reaction time. **D:** Maximum trajectory speed. **E:** Maximum force in the direction of movement. **F:** Trajectory path length.

## Experiment 3: Handle Viscous Resistance Center-Out Movement - age related performance

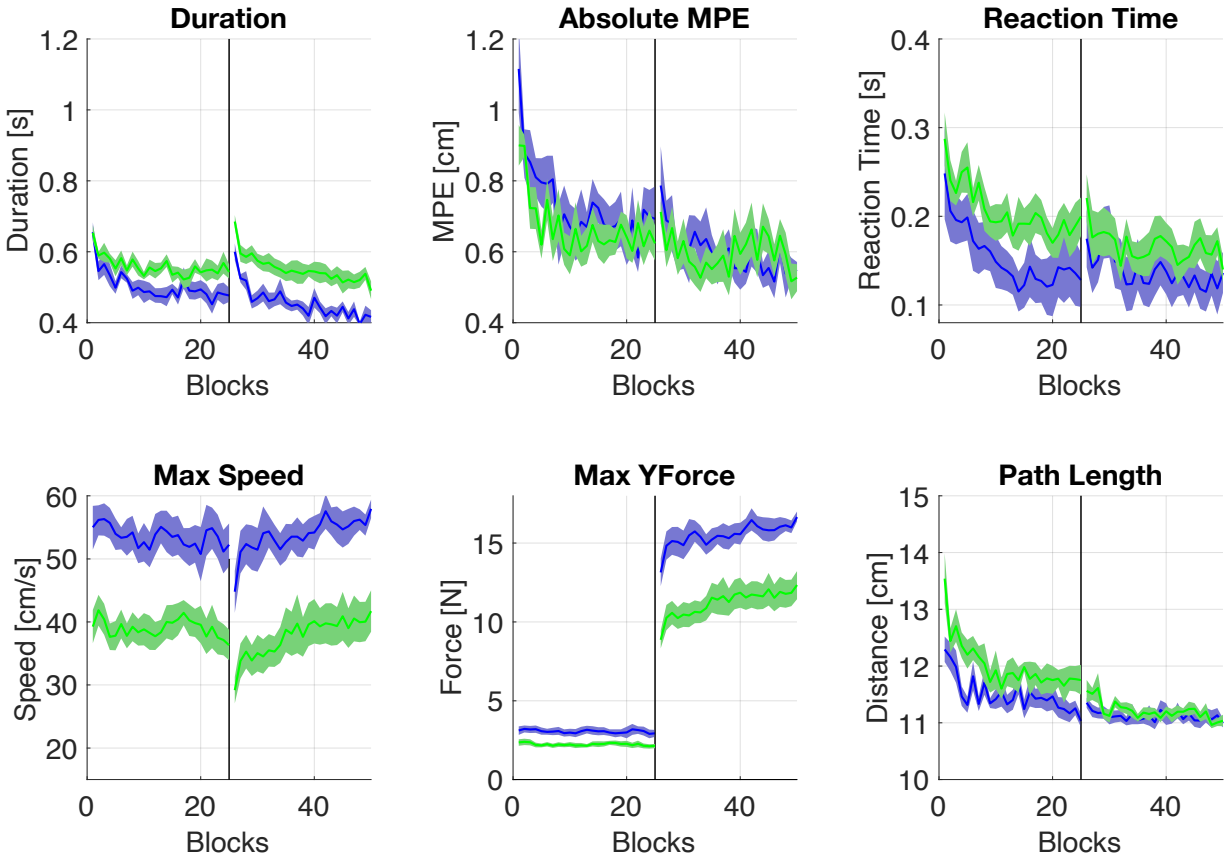


**Figure 8.** Movement metrics quantifying the hand trajectory during the right-hand null-viscous center-out task, plotted against blocks. Younger participants are shown in blue, and older participants in green. A: Movement duration. B: Absolute maximum perpendicular error (AMPE). C: Reaction time. D: Maximum trajectory speed. E: Maximum force in the direction of movement. F: Trajectory path length.

Participants again performed a right-hand center-out task involving 12 cm movements from a central start position to one of eight targets, under two conditions: a null field and a viscous field. The task comprised two phases of 200 trials each to assess performance in unloaded and loaded movements.

Younger adults generally made faster, shorter-duration movements, produced greater peak force in the movement direction, and had quicker reaction times. The dominant arm consistently showed superior performance, highlighting the metrics' sensitivity to individual differences in motor ability.

Fig. 8 illustrates the performance of younger and older participants across multiple metrics that characterize hand trajectories during the null-viscosity center-out task. Relative to the older group, younger participants complete the movements more quickly, exhibit shorter reaction times, reach higher peak speeds, apply greater force in the movement direction, and follow shorter paths. In contrast, AMPE remains comparable between the two groups

Repeated-measures ANOVAs were used to examine the significance of differences in the measured metrics between pairs of blocks (16 trials each) located at the initial null exposure, final null exposure, initial viscous dynamic exposure, and final viscous dynamic exposure. Post hoc comparisons were conducted to further assess significant differences between these phases.

Significant phase effects were observed across most metrics in both age groups. For younger participants, Duration, AMPE, Peak Y-Force, and Path Length showed consistent changes across all task phases. Reaction Time and Peak Speed also changed significantly over time, although Reaction Time was stable during the mass introduction phase. For older participants, strong effects were observed in Duration, AMPE, Peak Y-Force, and Path Length, with adaptation particularly evident between the null and mass dynamic phases. Reaction Time did not differ significantly across phases in this group. Notably, Peak Y-Force showed extremely large effect sizes in both groups ($\omega^2 > 0.85$), indicating a strong sensitivity to the dynamic manipulation. Detailed results are summarized in Table 5.

**Table 5.** Repeated-measures ANOVA results for each age group with post hoc comparisons: ANOVAs were conducted for each performance metric within each age group across three key phases of the task. Bonferroni-corrected post hoc comparisons are reported for: (1) initial vs final null blocks, (2) final null blocks vs introduction of the mass dynamic, and (3) start vs end of the mass dynamic blocks. Significant p-values are shown in bold.

| AGE GROUP | METRIC | F | P | $\omega^2$ | $P_{BONF}$ (1) | $P_{BONF}$ (2) | $P_{BONF}$ (3) |
|---|---|---|---|---|---|---|---|
| Younger | Duration | 48.947 | **< 0.001** | 0.463 | **< 0.001** | **< 0.001** | **< 0.001** |
| | AMPE | 50.677 | **< 0.001** | 0.510 | **< 0.001** | **0.001** | **0.002** |
| | Reaction Time | 18.853 | **< 0.001** | 0.201 | **0.005** | 0.987 | **0.034** |
| | Peak Speed | 18.361 | **< 0.001** | 0.096 | 0.098 | 0.002 | **< 0.001** |
| | Peak Y-Force | 250.107 | **< 0.001** | 0.855 | 0.059 | < 0.001 | **< 0.001** |
| | Path Length | 37.046 | **< 0.001** | 0.555 | **< 0.001** | < 0.001 | **< 0.001** |
| Older | Duration | 53.759 | **< 0.001** | 0.684 | **< 0.001** | 0.141 | **< 0.001** |
| | AMPE | 31.797 | **< 0.001** | 0.550 | **< 0.001** | 0.141 | **0.027** |
| | Reaction Time | 4.953 | **0.005** | 0.063 | 0.253 | 0.868 | 0.236 |
| | Peak Speed | 11.089 | **< 0.001** | 0.116 | 1.000 | **< 0.001** | **< 0.001** |
| | Peak Y-Force | 388.621 | **< 0.001** | 0.916 | **1.000** | **< 0.001** | **< 0.001** |
| | Path Length | 17.334 | **< 0.001** | 0.401 | **0.009** | 1.000 | **0.007** |

## Summary within age and conditions

For younger participants, Duration, AMPE, Reaction Time, and Path Length decreased significantly during the null phase. The introduction of the viscous dynamic led to significant increases in Duration, AMPE, Peak Y-Force, and Path Length, while Peak Speed decreased. By the end of the viscous phase, Duration, AMPE, Reaction Time, and Path Length had decreased again, while Peak Speed and Peak Y-Force increased.

For older participants, Duration and AMPE decreased significantly during the null phase. Duration increased with the viscous dynamic and then decreased again, while AMPE only decreased by the end. Peak Speed decreased with the dynamic and increased later, and Peak Y-Force increased throughout. Path Length decreased over both phases. Reaction Time showed no significant changes.

Younger participants showed more consistent adaptation across all measures, with significant changes at each phase, while older participants exhibited fewer significant changes, particularly in AMPE and Reaction Time, and showed less sensitivity to the introduction of the viscous dynamic. This suggests younger adults adapted more readily to both the removal and addition of dynamic forces.

**Cross age statistical analyses**

To investigate age-related differences in performance, we compared average values for each metric between younger and older participants using an ANOVA, analysing the first half of trials (1–200) and the second half (201–400) separately.

In Phase 1, significant age-related differences were found for Duration, Peak Speed, Peak Y-Force, and Path Length, with moderate to large effect sizes. In Phase 2, strong group differences were observed in Duration, Peak Speed, and Peak Y-Force, with large effect sizes ($\omega^2 > 0.47$). No significant differences were observed for AMPE, Reaction Time, or Path Length during this phase. Detailed results are summarized in Table 6.

**Table 6.** ANOVA results comparing younger and older participants within each experimental phase: Separate one-way ANOVAs were conducted for each performance metric in Phase 1 (P1, trials 1–200) and Phase 2 (P2, trials 201–400). Reported values include F-statistics, p-values, and effect sizes ($\omega^2$). Significant p-values are shown in bold.

| PHASE OF EXPERIMENT | METRIC | F | P | $\omega^2$ |
|---|---|---|---|---|
| P1 | Duration | 6.411 | **0.025** | 0.265 |
| | AMPE | 0.940 | 0.350 | 0.000 |
| | Reaction Time | 3.224 | 0.096 | 0.129 |
| | Peak Speed | 16.316 | **0.001** | 0.505 |
| | Peak Y-Force | 9.588 | **0.009** | 0.364 |
| | Path Length | 4.703 | **0.049** | 0.198 |
| P2 | Duration | 14.343 | **0.002** | 0.471 |
| | AMPE | 0.0004 | 0.984 | 0.000 |
| | Reaction Time | 0.844 | 0.375 | 0.000 |
| | Peak Speed | 17.613 | **0.001** | 0.526 |
| | Peak Y-Force | 18.594 | **< 0.001** | 0.540 |
| | *Path Length* | 0.688 | 0.422 | 0.000 |

**Summary cross age**

These qualitative results partially align with statistical analyses across the two age groups in the two phases, P1 and P2, of the experiments. Movement duration is significantly shorter in the younger participants ($p$ = 0.025 and $p$ = 0.002), who also exhibit higher peak movement speed, (p = 0.001 and p = 0.001) and greater force in the direction of motion, ($p$ = 0.009 and p < 0.001). Path length is also significantly different in P1 (p = 0.049) No other metrics showed a statistically significant difference between the two age groups.

## Experiment 3: Handle Viscous Resistance Center-Out Movement - Comparison Between Hands.

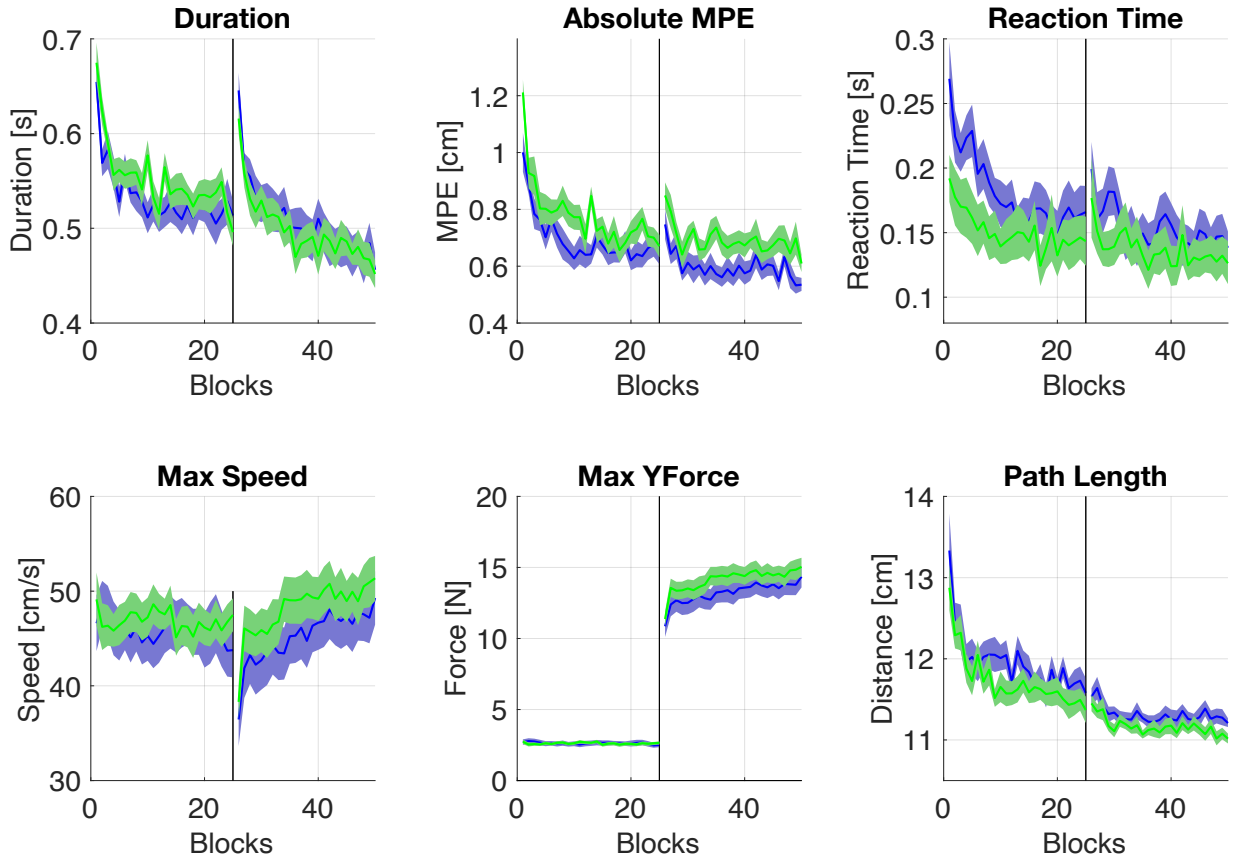


**Figure 9.** Movement metrics quantifying the hand trajectories during the null-viscous center-out task, plotted across blocks. The results from the experiments with participants using their right hand are shown in blue, and the corresponding results for the left-hand experiment are shown in green. A: Movement duration. B: Absolute maximum perpendicular error (MPE). C: Reaction time. D: Maximum trajectory speed. E: Maximum force in the direction of movement. F: Trajectory path length.

The experiment was then repeated with the left hand and a cross-hand comparison made. Fig. 9 shows the metrics across experimental trials, plotted as the mean ± SE. The most marked difference is that right-hand AMPE is notably lower than left-hand AMPE,

although there were also other differences. Left-hand peak speed was higher than right-hand peak speed, and left-hand path length was shorter. Statistical analyses confirm these observations.

To investigate differences in performance between the right and left hands, we compared average values for each metric between metrics using a repeated measures ANOVA, analysing the first half of trials (1 – 200) and the second half (201 – 400) separately.

In Phase 1, significant age-related differences were observed in AMPE, Reaction Time, and Path Length, with AMPE showing the largest effect ($\omega^2 = 0.133$). In Phase 2, AMPE, Reaction Time, and Path Length also reached significance, though with smaller effect sizes. No significant differences were found in Peak Speed or Peak Y-Force during either phase. Detailed results are summarized in Table 7.

**Table 7.** ANOVA results comparing younger and older participants within each experimental phase (third dataset): One-way ANOVAs were conducted separately for Phase 1 (P1, trials 1–200) and Phase 2 (P2, trials 201–400). The table reports F-values, p-values, and effect sizes ($\omega^2$). Significant p-values are shown in bold.

| PHASE OF EXPERIMENT | METRIC | F | P | $\omega^2$ |
|---|---|---|---|---|
| P1 | Duration | 3.021 | 0.106 | 0.056 |
| | AMPE | 10.167 | **0.007** | 0.133 |
| | Reaction Time | 14.011 | **0.002** | 0.047 |
| | Peak Speed | 0.059 | 0.811 | 0.000 |
| | Peak Y-Force | 0.143 | 0.712 | 0.000 |
| | Path Length | 4.853 | **0.046** | 0.036 |
| P2 | Duration | 0.004 | 0.949 | 0.000 |
| | AMPE | 9.138 | **0.010** | 0.151 |
| | Reaction Time | 5.104 | **0.042** | 0.012 |
| | Peak Speed | 2.115 | 0.170 | 0.005 |
| | Peak Y-Force | 3.514 | 0.083 | 0.010 |
| | Path Length | 7.618 | **0.016** | 0.069 |

### Summary cross hands

Right-hand AMPE values were significantly lower than left-hand values ($p = 0.007$ and $p=0.01$) and path lengths were significantly shorter ($p = 0.046$ and $p = 0.016$). No other metrics showed a statistically significant difference between the two hands. Reaction times were significantly shorter with the left hand ($p = 0.002$ and $p = 0.042$),

## Discussion (1582)

## The Effects of Aging on Sensorimotor Performance

In this study, we examine quantitative measures to test motor performance relevant to everyday tasks. We designed three experimental tasks using the vBOT robotic manipulandum (12), to accurately compare performance between healthy young adults (<35) and older adults (>60) in a controlled and repeatable fashion.

Across all three experiments, younger participants consistently demonstrated robust learning and adaptation in motor performance. They showed significant reductions in movement duration, Absolute Mean Position Error (AMPE), reaction time, and path length over the course of training, particularly in kinematic and viscous dynamic tasks. Younger individuals also adapted more consistently and quickly to the introduction of novel dynamics, such as added mass or viscous resistance, showing clear changes across all measured metrics. In comparison to older participants, younger adults had significantly shorter durations, higher peak speeds, greater directional force generation, and more extensive trajectory adjustments during the initial phases of exposure. These findings highlight a greater sensitivity to task dynamics and a higher capacity for motor adaptation among the younger cohort.

Analysis of right verses left-hand performance in Experiment 3 revealed significant asymmetries. AMPE and path length were both significantly lower for the right hand, indicating more accurate and efficient movements. In contrast, reaction times were significantly shorter with the left hand, possibly reflecting differences in motor planning or strategy rather than execution. No significant differences were found in peak speed or peak force between the hands. These hand-specific performance differences underscore the sensitivity and relevance of our methodology in capturing fine-grained variations in motor behavior. The ability to detect these subtle asymmetries demonstrates the utility of our approach for quantifying motor performance with high resolution and for identifying individual differences in motor control strategies.

The three experimental tasks differed significantly in their capacity to reveal age-related sensorimotor differences. Experiment 1, involving novel bimanual control of a virtual arm, highlighted initial difficulties among older adults in acquiring new motor skills, though performance improved significantly with practice. Experiment 2 assessed the management of inertial loads, clearly demonstrating older adults' reductions in peak forces and prolonged movement durations. However, Experiment 3, featuring viscous resistance and a scoring system designed to reward brisk movements, was particularly effective at differentiating younger from older adults. By explicitly encouraging participants to move quickly, the scoring mechanism appeared to push individuals closer to their limits, thereby likely exaggerating performance differences. Consequently, this task identified pronounced age-related deficits in force production, reaction time, and movement duration, suggesting its superior effectiveness for clinical assessment of subtle motor impairments associated with aging.

Our findings that movements take longer and slow down with age are consistent with previous research (17). Individual variability was found to be high, and some older adults performed similarly to younger adults. Variability may result from differences in lifestyle,

regular physical activity, cognitive engagement, or other unexplored genetic and environmental factors (18). As individuals age, sensorimotor performance often declines (18,19), impacting everyday activities such as drinking a glass of water or walking down the street (20). This decline is largely due to age-related alterations in the brain and body that affect motor control (21).

The decline in sensorimotor performance with aging is thought to arise from multifaceted neural mechanisms, primarily involving structural and functional changes within the central nervous system.

One of the most significant factors contributing to sensorimotor decline is a reduction in neuroplasticity - the brain's ability to adapt and reorganize in response to new experiences or environmental changes (22–24). Additionally, brain volume tends to decrease over time (25,26), which can impair the regulation of motor regions, further contributing to motor dysfunction (20).

One of the prominent neural changes is the progressive loss of gray matter volume, particularly affecting regions such as the motor cortex, basal ganglia, and cerebellum, which are critical for motor planning, execution, and coordination (20). Moreover, aging leads to reduced integrity of white matter tracts, including corticospinal and sensorimotor pathways, resulting in impaired signal conduction, reduced cortical excitability, and increased variability in motor responses (27). A reduction in neurotransmitter availability - particularly dopamine - further impairs motor control, reduces precision, and limits the adaptability of motor responses, thereby contributing significantly to sensorimotor deficits in older adults (28).

In addition to neural deterioration, biomechanical factors substantially exacerbate age-related sensorimotor decline. Aging is accompanied by progressive muscle atrophy (sarcopenia), characterized by reductions in muscle mass, strength, and contractile speed, which significantly impair motor function and reaction times (18). There is also a decline in proprioceptive acuity due to decreased density and sensitivity of peripheral sensory receptors (including muscle spindles and mechanoreceptors), impairing the ability to accurately sense joint position and movement—a capability crucial for precise motor control (29). Furthermore, increased joint stiffness and reduced flexibility, resulting from degenerative changes in connective tissues, limit movement range and fluidity, compounding sensorimotor impairment in older populations (30).

When motor function becomes further impaired by neurological diseases such as Parkinson's disease, stroke, or other movement disorders, abnormal movements such as tremors (31), bradykinesia (32), rigidity (33), or dyskinesia (34) become prevalent. These pathological conditions exaggerate the sensorimotor deficits already seen in healthy aging, introducing additional complexity for both assessment and rehabilitation (7,35). Such changes might explain the observed decline in sensorimotor performance.

## Current Clinical Paradigms

To assess human motor performance, several clinical paradigms have been developed. The clinical assessment “Timed Up & Go” (TUG) was designed as a brief evaluation of basic mobility skills in frail and older adults (36). During the test, participants are instructed to stand up, walk three meters to a chair, and then sit down again. This assessment has proven to be an effective tool for evaluating mobility, walking, and balance (37–39). Moreover, it has been demonstrated to be a reliable method for identifying adults at increased risk of falls (40).

For the upper body, there has been continuous research aimed at developing tests that evaluate multiple aspects of motor function. Researchers have specifically focused on creating clinical assessments for upper-limb motor abilities. To evaluate upper-limb motor function, researchers introduced the Wolf Motor Function Test (WMFT) (41), in which participants perform tasks that simulate daily activities, such as lifting or picking up objects. This test is widely used in hospitals, particularly for neurorehabilitation purposes (35,42,43). Other well-known assessments include the Action Research Arm Test (ARAT), which evaluates post-stroke patients by measuring grasp, grip, pinch, and other motor tasks (44). Another commonly used assessment is the Jebsen–Taylor Hand Function Test (JTHFT), also designed for post-stroke patients. This test is sensitive to changes over time, making it an effective tool for monitoring recovery (45).

Some tests assess both upper- and lower-limb movement. One example is the Fugl–Meyer Assessment (FMA), which is typically used to evaluate individuals with stroke or neurological impairments. It assesses balance and coordination in both the upper and lower extremities and is widely used in research and clinical settings (46).

### Robotic Manipulanda Assessment

The experimental results presented here demonstrate that the vBOT system, in conjunction with the experimental procedures, can detect subtle changes in performance caused by age.

Previous research employing robotic manipulanda to assess sensorimotor ability has predominantly used standardized upper-limb reaching tasks designed to objectively evaluate specific aspects of motor and sensory function. Common movement paradigms include:

Center-out reaching tasks: Participants typically initiate movements from a central starting position to peripheral targets arranged radially around the starting point. These tasks assess motor accuracy, reaction time, movement speed, trajectory smoothness, and force control (10,47).

Visuomotor adaptation paradigms: Participants perform reaching movements under altered visual feedback (e.g., rotated cursor) or novel force environments (e.g., viscous, inertial, or perturbation fields). Such tasks evaluate sensory integration, adaptation, learning rates, and the ability to generalize learned sensorimotor mappings (4,48,49).

Bimanual coordination tasks: Tasks requiring simultaneous or coordinated movements of both arms have been used to investigate interlimb coordination, sensorimotor integration, and neural control mechanisms underlying complex motor behavior (50,51).

Proprioceptive assessment paradigms: Robotic manipulanda have been used to passively move a participant's limb to specific positions, after which participants are asked to reproduce or discriminate limb positions. These paradigms quantify proprioceptive acuity, position sense, and kinesthetic deficits in both neurological disorders and aging populations (7,8).

Force generation and control tasks: Participants are asked to exert specified forces or match force profiles, either statically or dynamically. These tasks measure maximum voluntary force, accuracy of force modulation, and motor deficits related to muscle weakness or impaired neuromuscular control (11).

Collectively, these paradigms enable detailed, quantitative assessments of various components of sensorimotor function, providing insights into motor control deficits, adaptation processes, and sensory impairments associated with aging, neurological disease, or injury. However, in cases of severe movement disruption—where patients may have difficulty initiating movement or are unable to perform certain tasks—additional or alternative metrics may be necessary to accurately assess functional capacity and impairment.

Compared to widely-used clinical assessments such as WMFT or ARAT, the robotic approach provides finer resolution and greater sensitivity, especially in detecting subtle deficits or tracking small changes over short intervals Clinically, the proposed robotic tasks could be implemented in outpatient rehabilitation settings, allowing practitioners to routinely quantify subtle sensorimotor deficits, monitor progression, and evaluate treatment efficacy.

Emerging methods using robotic manipulanda, as utilized in this study, offer highly sensitive, quantitative assessments capable of detecting subtle impairments and characterizing abnormal movement patterns (47). Future developments in robotic technologies combined with machine learning algorithms could further enhance diagnostic accuracy, enable precise tracking of disease progression, and allow personalized rehabilitation interventions tailored to the individual's specific sensorimotor impairments (11).

## Conclusions (201)

This study demonstrates that robotic manipulanda, specifically the vBOT (12) can be used to sensitively and quantitatively assess age-related differences in sensorimotor control. Across three experimental tasks, older adults consistently exhibited deficits in movement timing, force generation, and reaction speed, although some individual variability was observed. The use of both unimanual and bimanual paradigms enabled detailed characterization of performance, including lateralized differences between dominant and non-dominant limbs.

Our results reinforce the growing consensus that robotic systems can complement traditional clinical assessments by providing objective, high-resolution data on motor function. Such tools offer considerable promise for early detection of motor decline, tracking disease progression, and the development of rehabilitation interventions.

We note that our proof-of-concept study involved participants who were physically fit, particularly among the older participant group. This represents a sample skewed towards higher-functioning individuals. As a result, the observed differences between younger and older adults were probably smaller than those that would be seen in a clinical setting with less able patients. Obtaining more representative participant samples will be a priority in future research. Further studies should also include more diverse participant groups and explore how robotic assessments can be integrated into clinical workflows for both age-related and neurological conditions.

## Supplementary Material

The supplementary material presents the experimental data in an alternative format.

## Disclosures

The authors declare that they have no financial, personal, or professional conflicts of interest that may have influenced the content of this paper.

## Author Contributions

LAH, ISH, GS, and EE conceived the study. LAH and ISH implemented the study, and LAH conducted data collection. Data analysis was carried out by LAH and ISH. The initial draft of the manuscript was written by LAH. All authors - LAH, ISH, GS, and EE - reviewed and edited the manuscript.

## References


1. Grinin L, Grinin A, Korotayev A. Global Aging and our Futures. World Futur. 2023 Jul 4;79(5):536–56.

2. WHO Global. Ageing and health. 2024 [cited 2024 Dec 17]. Ageing and health. Available from: https://www.who.int/news-room/fact-sheets/detail/ageing-and-health

3. Hogan N, Krebs HI, Charnnarong J, Srikrishna P, Sharon A. MIT-MANUS: a workstation for manual therapy and training. I. In: [1992] Proceedings IEEE International Workshop on Robot and Human Communication [Internet]. 1992 [cited 2024 Mar 25]. p. 161–5. Available from: https://ieeexplore.ieee.org/abstract/document/253895

4. Scott SH. Apparatus for measuring and perturbing shoulder and elbow joint positions and torques during reaching. J Neurosci Methods. 1999 Jul 15;89(2):119–27.

5. Krebs HI, Volpe BT, Aisen ML, Hogan N. Increasing productivity and quality of care: robot-aided neuro-rehabilitation. J Rehabil Res Dev. 2000;37(6):639–52.

6. Krebs HI, Hogan N. Therapeutic Robotics: A Technology Push. Proc IEEE Inst Electr Electron Eng. 2006 Sep 1;94(9):1727–38.

7. Dukelow SP, Herter TM, Moore KD, Demers MJ, Glasgow JI, Bagg SD, et al. Quantitative assessment of limb position sense following stroke. Neurorehabil Neural Repair. 2010 Feb;24(2):178–87.

8. Herter TM, Scott SH, Dukelow SP. Systematic changes in position sense accompany normal aging across adulthood. J Neuroengineering Rehabil. 2014 Mar 25;11:43.

9. Kitchen NM, Miall RC. Proprioceptive deficits in inactive older adults are not reflected in fast targeted reaching movements. Exp Brain Res. 2019 Feb 1;237(2):531–45.

10. Bosecker C, Dipietro L, Volpe B, Krebs HI. Kinematic robot-based evaluation scales and clinical counterparts to measure upper limb motor performance in patients with chronic stroke. Neurorehabil Neural Repair. 2010 Jan;24(1):62–9.

11. Coderre AM, Zeid AA, Dukelow SP, Demmer MJ, Moore KD, Demers MJ, et al. Assessment of upper-limb sensorimotor function of subacute stroke patients using visually guided reaching. Neurorehabil Neural Repair. 2010;24(6):528–41.

12. Howard IS, Ingram JN, Wolpert DM. A modular planar robotic manipulandum with end-point torque control. J Neurosci Meth. 2009;181(2):199–211.

13. Oldfield RC. The assessment and analysis of handedness: The Edinburgh inventory. Neuropsychologia. 1971 Mar 1;9(1):97–113.

14. Howard IS, Alvarez-Hidalgo L. Haptic Force Feedback Enhances de Novo Learning of Arm Kinematics and Dynamics [Internet]. bioRxiv; 2025 [cited 2025 May 10]. p. 2025.04.29.651298. Available from: https://www.biorxiv.org/content/10.1101/2025.04.29.651298v1

15. Scheidt RA, Reinkensmeyer DJ, Conditt MA, Rymer WZ, Mussa-Ivaldi FA. Persistence of motor adaptation during constrained, multi-joint, arm movements. J Neurophysiol. 2000 Aug;84(2):853–62.

16. JASP Team. JASP (Version 0.19.0)[Computer software] [Internet]. 2024. Available from: https://jasp-stats.org/

17. Moulton RH, Rudie K, Dukelow SP, Scott SH. Quantitatively assessing aging effects in rapid motor behaviours: a cross-sectional study. J NeuroEngineering Rehabil. 2022 Jul 26;19(1):82.

18. Hunter SK, Pereira HM, Keenan KG. The aging neuromuscular system and motor performance. J Appl Physiol. 2016 Oct;121(4):982–95.

1099 19. Yoshimura N, Tsuda H, Aquino D, Takagi A, Ogata Y, Koike Y, et al. Age-Related
1100 Decline of Sensorimotor Integration Influences Resting-State Functional Brain
1101 Connectivity. Brain Sci. 2020 Dec;10(12):966.

1102 20. Seidler RD, Bernard JA, Burutolu TB, Fling BW, Gordon MT, Gwin JT, et al. Motor
1103 control and aging: Links to age-related brain structural, functional, and biochemical
1104 effects. Neurosci Biobehav Rev. 2010 Apr 1;34(5):721–33.

1105 21. Clark BC, Taylor JL. Age-related changes in motor cortical properties and voluntary
1106 activation of skeletal muscle. Curr Aging Sci. 2011 Dec;4(3):192–9.

1107 22. Burke SN, Barnes CA. Neural plasticity in the ageing brain. Nat Rev Neurosci. 2006
1108 Jan;7(1):30–40.

1109 23. Kourosh-Arami M, Hosseini N, Komaki A. Brain is modulated by neuronal plasticity
1110 during postnatal development. J Physiol Sci. 2021 Nov 17;71(1):34.

1111 24. Marzola P, Melzer T, Pavesi E, Gil-Mohapel J, Brocardo PS. Exploring the Role of
1112 Neuroplasticity in Development, Aging, and Neurodegeneration. Brain Sci. 2023
1113 Dec;13(12):1610.

1114 25. Raz N, Gunning-Dixon F, Head D, Dupuis J, Acker J. Neuroanatomical correlates of
1115 cognitive aging: Evidence from structural magnetic resonance imaging.
1116 Neuropsychology. 1998 Feb 1;12:95–114.

1117 26. Fjell AM, Walhovd KB. Structural brain changes in aging: courses, causes and
1118 cognitive consequences. Rev Neurosci. 2010;21(3):187–221.

1119 27. Cassady K, Ruitenberg MFL, Reuter-Lorenz PA, Tommerdahl M, Seidler RD. Neural
1120 Dedifferentiation across the Lifespan in the Motor and Somatosensory Systems.
1121 Cereb Cortex N Y N 1991. 2020 May 18;30(6):3704–16.

1122 28. Kuehn E, Dinse J, Jakobsen E, Long X, Schäfer A, Bazin PL, et al. Body Topography
1123 Parcellates Human Sensory and Motor Cortex. Cereb Cortex N Y N 1991. 2017 Jul
1124 1;27(7):3790–805.

1125 29. Goble DJ, Coxon JP, Van Impe A, Geurts M, Doumas M, Wenderoth N, et al. Brain
1126 activity during ankle proprioceptive stimulation predicts balance performance in young
1127 and older adults. J Neurosci Off J Soc Neurosci. 2011 Nov 9;31(45):16344–52.

1128 30. Kulmala JP, Korhonen MT, Kuitunen S, Suominen H, Heinonen A, Mikkola A, et al.
1129 Which muscles compromise human locomotor performance with age? J R Soc
1130 Interface. 2014 Nov 6;11(100):20140858.

1131 31. Deuschl G, Bain P, Brin M. Consensus statement of the Movement Disorder Society
1132 on Tremor. Ad Hoc Scientific Committee. Mov Disord Off J Mov Disord Soc. 1998;13
1133 Suppl 3:2–23.

32. Berardelli A, Rothwell JC, Thompson PD, Hallett M. Pathophysiology of bradykinesia in Parkinson's disease. Brain J Neurol. 2001 Nov;124(Pt 11):2131–46.

33. Fearon C, Doherty L, Lynch T. How Do I Examine Rigidity and Spasticity? Mov Disord Clin Pract. 2015;2(2):204–204.

34. Jankovic J. Motor fluctuations and dyskinesias in Parkinson's disease: Clinical manifestations. Mov Disord. 2005;20(S11):S11–6.

35. Edwards DF, Lang CE, Wagner JM, Birkenmeier R, Dromerick AW. An Evaluation of the Wolf Motor Function Test in Motor Trials Early After Stroke. Arch Phys Med Rehabil. 2012 Apr 1;93(4):660–8.

36. Podsiadlo D, Richardson S. The Timed "Up & Go": A Test of Basic Functional Mobility for Frail Elderly Persons. J Am Geriatr Soc. 1991 Feb;39(2):142–8.

37. Shumway-Cook A, Brauer S, Woollacott M. Predicting the Probability for Falls in Community-Dwelling Older Adults Using the Timed Up & Go Test. Phys Ther. 2000 Sep 1;80(9):896–903.

38. Ng SS, Hui-Chan CW. The Timed Up & Go Test: Its Reliability and Association With Lower-Limb Impairments and Locomotor Capacities in People With Chronic Stroke. Arch Phys Med Rehabil. 2005 Aug 1;86(8):1641–7.

39. Kristensen MT, Foss NB, Kehlet H. Timed "Up & Go" Test as a Predictor of Falls Within 6 Months After Hip Fracture Surgery. Phys Ther. 2007 Jan 1;87(1):24–30.

40. Nocera JR, Stegemöller EL, Malaty IA, Okun MS, Marsiske M, Hass CJ, et al. Using the Timed Up & Go test in a clinical setting to predict falling in Parkinson's disease. Arch Phys Med Rehabil. 2013 Jul;94(7):1300–5.

41. Wolf SL, Catlin PA, Ellis M, Archer AL, Morgan B, Piacentino A. Assessing Wolf motor function test as outcome measure for research in patients after stroke. Stroke. 2001 Jul;32(7):1635–9.

42. Fritz SL, Blanton S, Uswatte G, Taub E, Wolf SL. Minimal Detectable Change Scores for the Wolf Motor Function Test. Neurorehabil Neural Repair. 2009 Sep 1;23(7):662–7.

43. Turtle B, Porter-Armstrong A, Stinson M. The reliability of the graded Wolf Motor Function Test for stroke. Br J Occup Ther. 2020 Sep;83(9):585–94.

44. Lyle RC. A performance test for assessment of upper limb function in physical rehabilitation treatment and research. Int J Rehabil Res Int Z Rehabil Rev Int Rech Readaptation. 1981;4(4):483–92.

45. Jebsen RH, Taylor N, Trieschmann RB, Trotter MJ, Howard LA. An objective and standardized test of hand function. Arch Phys Med Rehabil. 1969 Jun;50(6):311–9.

46. Sullivan KJ, Tilson JK, Cen SY, Rose DK, Hershberg J, Correa A, et al. Fugl-Meyer assessment of sensorimotor function after stroke: standardized training procedure for clinical practice and clinical trials. Stroke. 2011 Feb;42(2):427–32.

47. Krebs HI, Hogan N, Aisen ML, Volpe BT. Robot-aided neurorehabilitation. IEEE Trans Rehabil Eng Publ IEEE Eng Med Biol Soc. 1998 Mar;6(1):75–87.

48. Shadmehr R, Mussa-Ivaldi FA. Adaptive representation of dynamics during learning of a motor task. J Neurosci. 1994 May 1;14(5):3208–24.

49. Cressman EK, Henriques DYP. Sensory recalibration of hand position following visuomotor adaptation. J Neurophysiol. 2009 Dec;102(6):3505–18.

50. Diedrichsen J. Optimal task-dependent changes of bimanual feedback control and adaptation. Curr Biol CB. 2007 Oct 9;17(19):1675–9.

51. Howard IS, Ingram JN, Wolpert DM. Composition and decomposition in bimanual dynamic learning. J Neurosci. 2008 Oct 15;28(42):10531–40.